Article

Cell Metabolism

Lack of Sterol Regulatory Element Binding Factor-1c Imposes Glial Fatty Acid Utilization Leading to Peripheral Neuropathy

Graphical Abstract

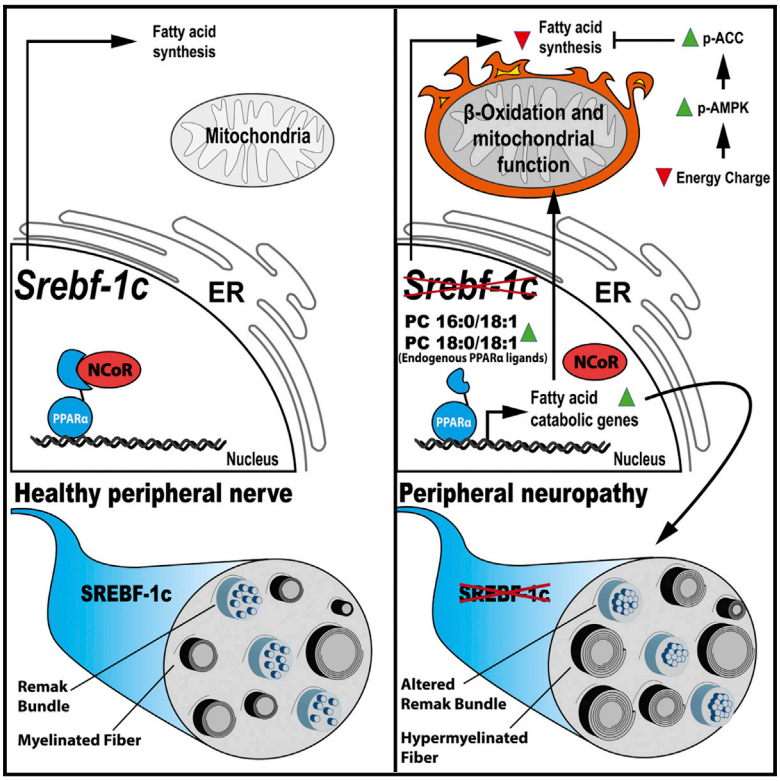

Highlights

- *Srebf1c* KO mice have blunted nerve FA synthesis and develop peripheral neuropathy
- Reduced nerve FA synthesis results in accretion of Pparα ligands in Schwann cells
- Increased Pparα signaling in peripheral nerves alters myelin structure/function
- Treatment with a Pparα antagonist rescues the neuropathy of *Srebf1c* KO mice

Authors

Gaia Cermenati, Matteo Audano, ..., Donatella Caruso, Nico Mitro

Correspondence

donatella.caruso@unimi.it (D.C.), nico.mitro@unimi.it (N.M.)

In Brief

Cermenati et al. look at the specific role of fatty acid synthesis in peripheral neuropathy and show that loss of *Srebf1c* not only results in decreased fatty acid synthesis but also increased fatty acid oxidation due to increased Pparα activity. Pparα antagonist treatment rescues the neuropathy of *Srebf1c*-null mice.

Cermenati et al., 2015, Cell Metabolism *21*, 571–583
April 7, 2015
http://dx.doi.org/10.1016/j.cmet.2015.02.016

Cell Metabolism
Article

Lack of Sterol Regulatory Element Binding Factor-1c Imposes Glial Fatty Acid Utilization Leading to Peripheral Neuropathy

Gaia Cermenati,[1] Matteo Audano,[1] Silvia Giatti,[1] Valentina Carozzi,[2] Carla Porretta-Serapiglia,[3] Emanuela Pettinato,[4] Cinzia Ferri,[4] Maurizio D'Antonio,[4] Emma De Fabiani,[1] Maurizio Crestani,[1] Samuele Scurati,[5] Enrique Saez,[6] Iñigo Azcoitia,[7] Guido Cavaletti,[2] Luis-Miguel Garcia-Segura,[8] Roberto C. Melcangi,[1] Donatella Caruso,[1,*] and Nico Mitro[1,*]

[1]DiSFeB, Dipartimento di Scienze Farmacologiche e Biomolecolari, Università degli Studi di Milano, Milano, 20133, Italy
[2]Experimental Neurology Unit, Department of Surgery and Translational Medicine, Università degli Studi Milano-Bicocca, Monza, 20052, Italy
[3]IRCCS Foundation, Carlo Besta Neurological Institute, Milano, 20133, Italy
[4]Division of Genetics and Cell Biology, IRCCS San Raffaele Scientific Institute, DIBIT, Milano, 20132, Italy
[5]DASP s.r.l., Gerenzano, 21040, Italy
[6]Department of Chemical Physiology, The Scripps Research Institute, La Jolla, CA 92037, USA
[7]Departamento de Biología Celular, Facultad de Biología, Universidad Complutense de Madrid, Madrid, E-28040, Spain
[8]Instituto Cajal, C.S.I.C., Madrid, E-28002, Spain
*Correspondence: donatella.caruso@unimi.it (D.C.), nico.mitro@unimi.it (N.M.)
http://dx.doi.org/10.1016/j.cmet.2015.02.016

SUMMARY

Myelin is a membrane characterized by high lipid content to facilitate impulse propagation. Changes in myelin fatty acid (FA) composition have been associated with peripheral neuropathy, but the specific role of peripheral nerve FA synthesis in myelin formation and function is poorly understood. We have found that mice lacking sterol regulatory element-binding factor-1c (*Srebf1c*) have blunted peripheral nerve FA synthesis that results in development of peripheral neuropathy. *Srebf1c*-null mice develop Remak bundle alterations and hypermyelination of small-caliber fibers that impair nerve function. Peripheral nerves lacking *Srebf1c* show decreased FA synthesis and glycolytic flux, but increased FA catabolism and mitochondrial function. These metabolic alterations are the result of local accumulation of two endogenous peroxisome proliferator-activated receptor-α (Pparα) ligands, 1-palmitoyl-2-oleyl-*sn*-glycerol-3-phosphatidylcholine and 1-stearoyl-2-oleyl-*sn*-glycerol-3-phosphatidylcholine. Treatment with a Pparα antagonist rescues the neuropathy of *Srebf1c*-null mice. These findings reveal the importance of peripheral nerve FA synthesis to sustain myelin structure and function.

INTRODUCTION

Peripheral neuropathies belong to a heterogeneous group of disorders that negatively impact the function of one or more peripheral nerves. The incidence of peripheral neuropathies, which can be either inherited or acquired, is 2.4% in the general population and 8% in older adults (Hughes, 2002). One mechanism that has been proposed to explain the pathogenic basis of incapacitating peripheral neuropathies is the inability of Schwann cells to properly assemble and/or maintain nervous system myelin (Roglio et al., 2008; Saher et al., 2009; Verheijen et al., 2009; Viader et al., 2013). Schwann cells constitute the glia of the peripheral nervous system. In response to axonal signal neuregulin-1 (NRG1) type III (Taveggia et al., 2005) or, in the case of nerve injury, NRG1 type I (Stassart et al., 2013), Schwann cells distinguish larger axons to build or regenerate myelin. Schwann cells also associate with several unmyelinated small-diameter sensory axons and surround them to form Remak bundles.

Myelin is a specialized membrane highly enriched in lipids that provide the electrical insulation properties to allow efficient propagation of neuronal action potentials. The most abundant lipids in peripheral nervous system myelin are cholesterol and fatty acids (FAs), the latter being conjugated to different families of phospholipids and glycosphingolipids (Garbay et al., 2000). Disorders in cholesterol metabolism (Correa-Cerro et al., 2006; Fitzky et al., 2001; Pollock et al., 1983; Saher et al., 2009; Wassif et al., 2001) and FA accumulation in peroxisomes (Kassmann et al., 2007; Van Veldhoven, 2010; Wierzbicki et al., 2002) have been associated with defects in myelin function. Moreover, FAs have been shown to influence the biophysical properties of myelin, and changes in the FA composition of myelin can alter peripheral nerve myelin structure and function (Cermenati et al., 2012; Verheijen et al., 2009).

Lipid synthesis is under the control of three different transcription factors of the basic helix-loop-helix-leucine zipper family referred to as sterol regulatory element-binding factors (Srebfs) (Horton et al., 2002). Srebf2 is an activator of cholesterol biosynthesis, while Srebf1a and Srebf1c, derived from a single gene via alternate forms of exon 1, regulate cholesterol, FA, and triglyceride synthesis (Liang et al., 2002). It is thought that Srebf1c, which contains a shorter and weaker transcriptional activation domain relative to Srebf1a, is an isoform that preferentially governs FA and triglyceride synthesis (Liang et al., 2002). Loss of expression of all three Srebf isoforms specifically in Schwann cells results in

hypomyelination and neuropathy, demonstrating the vital role of lipid synthesis in peripheral nerve structure and function (Verheijen et al., 2009). Interestingly, FAs required for myelin formation can be either synthesized endogenously or slowly taken up from the circulation or from other nerve compartments (Bourre et al., 1987; Verheijen et al., 2003, 2009; Yao et al., 1980). This latter observation raises the question of whether endogenous FA synthesis is necessary to sustain myelin formation, maintain nerve integrity, and thus protect against the development of peripheral neuropathy. Although the role of altered cholesterol metabolism in peripheral neuropathy is well established (Saher et al., 2011), the specific contribution of FA synthesis remains poorly understood.

Here, we explored the extent to which lack of the key lipogenic transcription factor *Srebf1c* could result in the development of peripheral neuropathy. Using functional, morphological, and morphometric analyses, we found that *Srebf1c*-null mice display a neuropathic phenotype consisting in hypermyelinated small-caliber fibers, the result of changes in myelin periodicity. Unexpectedly, transcriptomics and metabolomics revealed activation of peroxisome proliferator-activated receptor α (Pparα) signaling in Schwann cells as a result of increased levels of two distinct physiological Pparα ligands, 1-palmitoyl-2-oleyl-*sn*-glycerol-3-phosphatidylcholine (PC-C16:0/C18:1) and 1-stearoyl-2-oleyl-*sn*-glycerol-3-phosphatidylcholine (PC-C18:0/C18:1) (Chakravarthy et al., 2009; Liu et al., 2013). Pparα is a nuclear receptor that directs uptake, utilization, and catabolism of FAs by increasing expression of genes involved in FA transport, binding and activation, and peroxisomal and mitochondrial FA β-oxidation (Bantubungi et al., 2012; Kersten et al., 1999). As a consequence of abnormal local Pparα activation, *Srebf1c*-null Schwann cells exhibit increased FA utilization, a detrimental condition that ultimately results in the development of peripheral neuropathy.

RESULTS

Srebf1c-Null Mice Develop Peripheral Neuropathy

To explore the extent to which reduced FA synthesis affects myelin structure and function and contributes to peripheral neuropathy, we used mice lacking the major lipogenic transcription factor *Srebf1c* (Liang et al., 2002). Full-body *Srebf1c* knockout (KO) mice were studied at 2 and 10 months of age to evaluate the development of peripheral neuropathy over time and in the fed state to maximize expression of *Srebf1c* in wild-type mice (Liang et al., 2002). Body weight and glycemia were unchanged at either age (Figures S1A, S1B, S1M, and S1N), but circulating total cholesterol and triglycerides were significantly decreased in *Srebf1c*-null mice relative to wild-type littermates at both 2 and 10 months of age (Figures S1C, S1D, S1O, and S1P). RNA and protein analyses showed that Srebf1c was virtually absent in the sciatic nerve of KO mice (Figures S1S and S1T). These studies also confirmed previous reports (de Preux et al., 2007) indicating that *Srebf1c* is the main isoform expressed in peripheral nerves (Figure S1S).

To evaluate the presence of peripheral neuropathy in *Srebf1c* KO mice, we used a battery of functional and morphological/morphometric analyses. Thermal and mechanical nociceptive threshold were both decreased at 2 and 10 months of age in *Srebf1c*-null mice (Figures S1E, S1F, 1A, and 1B), whereas nerve conduction velocity (NCV) and intraepidermal nerve fiber (IENF) density were reduced only at 10 months of age (Figures 1C, 1D, S1G, and S1H). Nerves from mice lacking *Srebf1c* did not show fiber loss (Figures S1I and S1Q) or myelin infoldings (Figures S1J and S1R). Similar to some forms of human peripheral neuropathy (Kennedy et al., 1996) and peripheral neuropathy in other animal models (Viader et al., 2013), *Srebf1c*-null mice at 2 months of age showed subtle abnormalities of small unmyelinated C fibers (Figure S1K) while myelin was unaltered (Figure S1L). Myelinating dorsal root ganglia (DRG)/Schwann cell explant cultures from wild-type and *Srebf1c* KO mice indicated that both genotypes myelinated in vitro to a similar extent (Figures S2A and S2B). At 10 months of age, *Srebf1c* KO sciatic nerves showed decreased *g* ratio of small-caliber fibers (1–4 μm axon diameter), indicating a selective hypermyelination (Figures 1E and 1F). Large-caliber fibers exhibited no substantial changes (Figure 1F). To better characterize the observed hypermyelination, we evaluated myelin periodicity, for hypermyelination can be due to increased membrane compaction or to packing defects that lead to myelin instability. *Srebf1c* KO sciatic nerves showed expanded myelin periodicity relative to wild-type nerves (Figure 1G). In addition, we detected decreased levels of the structural protein Pmp22 (Figure S2C) along with a slight increase in Remak bundle alterations (Figure 1H). Together, these findings establish a requirement for Srebf1c activity to maintain peripheral nerve structure and function.

Lack of *Srebf1c* Alters Metabolism and Decreases Peripheral Nerve FA Synthesis

To probe the mechanism responsible for the nerve pathology observed in *Srebf1c* KO mice, we performed transcriptome analysis on 10-month-old mice, the age at which defects in nerve structure and function are most evident. Gene ontology analysis revealed that the majority of differentially regulated genes belonged to metabolic processes, specifically lipid, carbohydrate, and protein metabolism (Figure 2A). As expected, absence of *Srebf1c* resulted in decreased expression of FA biosynthesis genes (Figure 2B). In addition, we also found decreased expression of glycolytic genes. In contrast, expression of genes involved in FA catabolism, the tricarboxylic acid (TCA) cycle, mitochondrial function, and the unfolded protein response (UPR) was unexpectedly increased (Figure 2B). Validation of a series of genes involved in FA synthesis (Figure 2C) and quantification of total FAs (Figure 2D) confirmed the downregulation of this pathway in sciatic nerve, while total cholesterol levels were unaffected (Figure 2E). Notably, the amount of palmitic acid (C16:0), the product of FA synthase (*Fasn*), was decreased in *Srebf1c* KO sciatic nerve. Stearic acid (C18:0) and oleic acid (C18:1), the substrate and product of stearoyl-CoA desaturase 1 (*Scd1*, a direct transcriptional target of *Srebf1c*) were respectively increased (C18:0) and decreased (C18:1), in line with the expression profile of *Scd1* (Figure 2D). To establish the specificity of these lipid synthesis defects, total FAs were quantified in liver. In spite of reduced expression of FA biosynthetic genes (Figure S3B), the levels of hepatic C16:0, a hallmark of endogenous FA synthesis, were unchanged (Figure S3A). In addition, the relative abundance of other FAs analyzed showed a different profile from that observed in sciatic nerve (Figure S3A). These

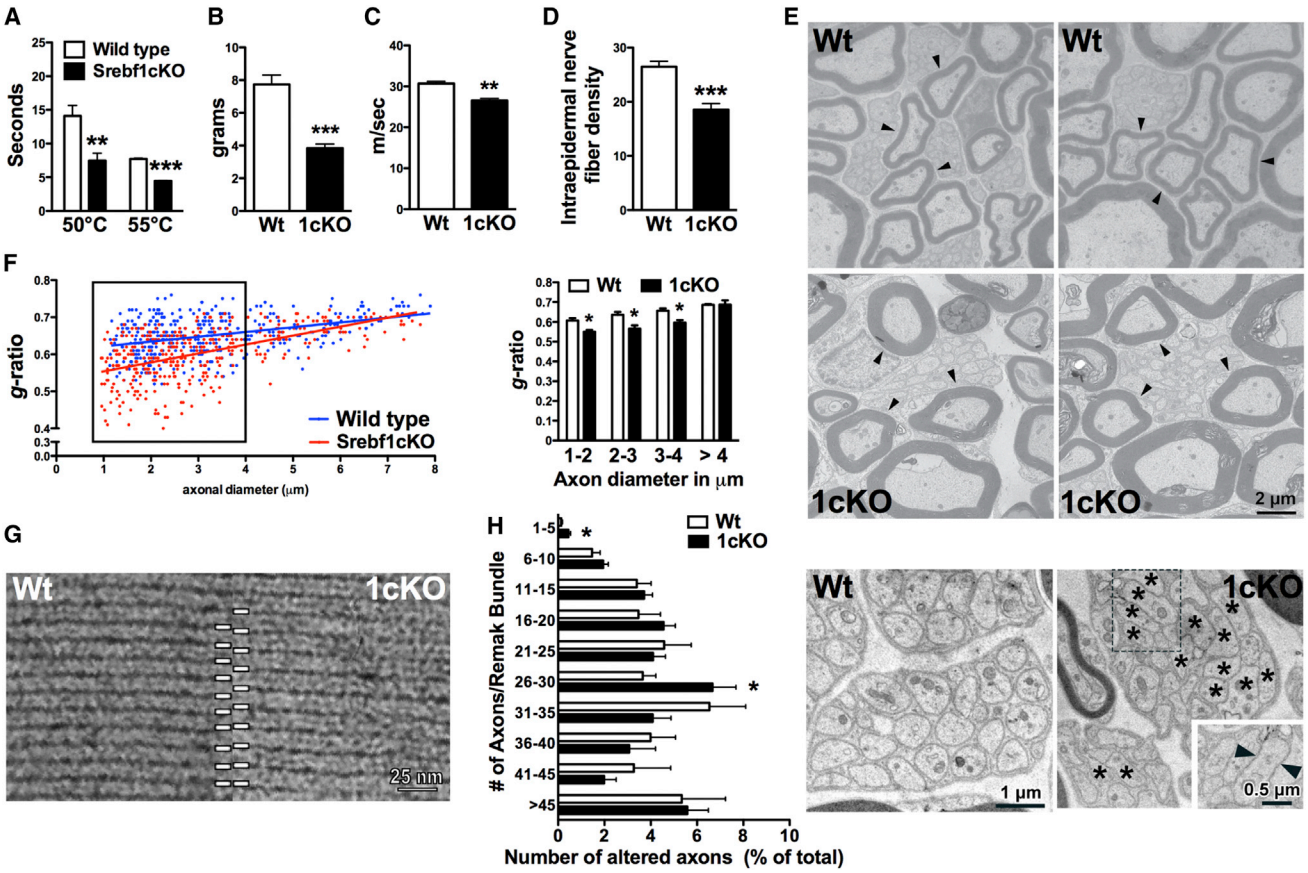

Figure 1. 10-Month-Old *Srebf1c* KO Mice Exhibit Peripheral Neuropathy

(A and B) Thermal and mechanical nociceptive threshold (n = 5 per group).

(C) NCV (n = 4 per group).

(D) IENF density (n = 5 per group).

(E) Representative images of small-caliber, hypermyelinated fibers in *Srebf1c* KO sciatic nerve. Arrows indicate hypermyelinated *Srebf1c* KO axons compared to similar axons in wild-type sciatic nerve.

(F) *g* ratio of sciatic nerve myelinated fibers and quantification accounting for axon diameter. The square indicates small-caliber fibers (<4 μm).

(G) Ultra structural analysis of myelin periodicity shows that myelin sheaths are compacted but that the periodicity is enlarged in *Srebf1c* KO nerves. White bars indicate ten major dense lines equal to nine periods.

(H) Quantification of altered axons per Remak bundle binned into groups and shown as a percentage of total axons. Representative figure of Remak bundles in sciatic nerves. Asterisks indicate Remak bundle alterations. Inset shows lack of Schwann cell cytoplasm between altered axons indicated by black arrows. Data are expressed as mean ± SEM and are representative of three experiments. p values determined by unpaired student's t test. *$p < 0.05$, **$p < 0.01$, and ***$p < 0.001$ versus wild-type.

observations may be explained by the fed state of the mice and by the primary exposure of the liver to nutritional cues leading to increased uptake of FAs present in the diet. Consistent with this notion, increased levels of the essential FA linoleic acid (C18:2) were observed in the liver (Figure S3A) but not in the sciatic nerve (Figure 2D) of *Srebf1c* KO mice. Collectively, these observations corroborate the role of Srebf1c as a major lipogenic transcription factor regulating FA synthesis in peripheral nerves whose absence modifies metabolic gene expression.

Enhanced Oxidative Metabolism in *Srebf1c* KO Nerves

Because transcriptome analysis indicated that genes involved in FA catabolism, the TCA cycle, and mitochondrial function were upregulated in 10-month-old *Srebf1c* KO nerves (Figure 2B), we evaluated the energy status of wild-type and *Srebf1c* KO sciatic nerves. The levels of ATP, ADP, and AMP were all increased in *Srebf1c* KO nerves (Figure 3A). More importantly, the adenylate energy charge, an index of the energy status of cells (Atkinson and Walton, 1967), was significantly reduced in *Srebf1c* KO nerves (Figure 3A). The observed energy depletion was confirmed by analysis of the phosphorylation status of the energy sensor AMP-activated protein kinase (Ampk). Ampk is activated by increases in the AMP/ATP ratio and phosphorylation at threonine 172, a marker of its activation (Hardie et al., 2012). We detected increased Ampk phosphorylation relative to total Ampk levels in the sciatic nerves of *Srebf1c* KO mice (Figure 3B). In contrast, the liver in a fed state neither showed different levels of ATP nor changes in Ampk phosphorylation status, confirming that nerves lacking *Srebf1c* specifically experienced energy depletion (Figures S3C and S3D). As a readout

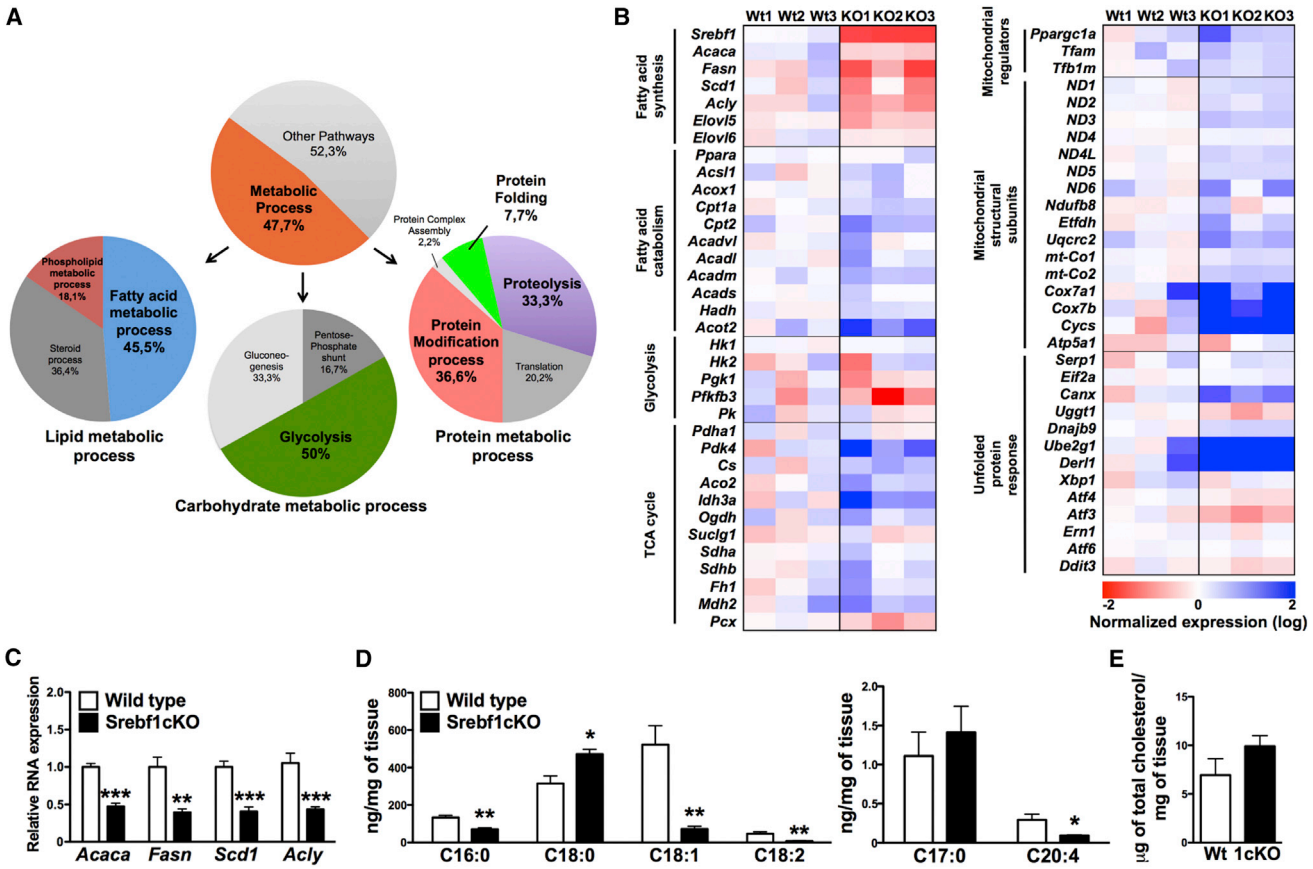

Figure 2. Gene Expression Impact of *Srebf1c* Deletion in 10-Month-Old Sciatic Nerve

(A) Gene ontology analysis of biological processes of differentially regulated genes in *Srebf1c* KO sciatic nerve.

(B) Heat map shows differentially expressed genes belonging to metabolic pathways most affected in *Srebf1c* KO sciatic nerve (n = 3).

(C) qRT-PCR analysis of *Acaca*, *Fasn*, *Scd1*, and *Acly* mRNA expression in sciatic nerves (n = 6 per group).

(D and E) Quantification of FAs and cholesterol in sciatic nerve (n = 5 per group). Data are expressed as mean ± SEM. p values determined by unpaired Student's t test. *p < 0.05, **p < 0.01, and ***p < 0.001 versus wild-type.

of increased Ampk activity, we measured phosphorylation levels of serine 79 of acetyl-CoA carboxylase alpha (Acaca), a classic downstream target of this energy sensor (Hardie et al., 2012). *Acaca* expression was decreased in *Srebf1c* KO nerves (Figure 2C), and total protein levels followed this trend; however, Acaca serine 79 phosphorylation was greater in KO sciatic nerves (Figure 3B). Inactivation of Acaca by phosphorylation is linked to a shift in FA metabolism from synthesis toward oxidation. Accordingly, expression of genes involved in FA β-oxidation and FA uptake and transport were upregulated in *Srebf1c* KO nerves (Figures 3C and S2D), indicating a boost in FA catabolism. As further evidence of induced, active FA β-oxidation (Koves et al., 2008), we found that the levels of short-chain acylcarnitines were increased in KO nerves (Figure 3D). The C2/C0 ratio (an index of β-oxidation of even number FAs) and the C2+C3/C0 ratio (an index of β-oxidation of odd number FAs) were both increased demonstrating a flux of FA β-oxidation toward acetyl-CoA formation and entry into the TCA cycle (Figure 3E). These data are substantiated by an increase in the NAD^+/NADH ratio (Figure 3F) and by enhanced expression of genes involved in the TCA cycle (Figure 3C). In contrast, the liver profile of acylcarnitines levels (Figure S4A) and FA catabolism and TCA cycle gene expression were largely unchanged or decreased (Figure S3B).

FA catabolism in peripheral nerve is dependent on mitochondrial function (Viader et al., 2013) and 10-month-old *Srebf1c* KO nerves showed increased mitochondrial DNA content, a hallmark of mitochondrial biogenesis (Figure 4A). Furthermore, the expression of transcription factors that regulate mitochondrial function and that of structural subunits of the electron transport chain (ETC) were increased at both the mRNA and protein levels (Figures 4B and 4C). As evidence of increased mitochondrial activity, we detected increased overall respiration coupled to oxidative phosphorylation in *Srebf1c* KO sciatic nerves (Figure 4D). In addition, the activities of ETC complex I, II, and IV were generally increased although only those of complex I and IV reached statistical significance (Figure 4D). Increased mitochondrial activity is often coupled to the generation of reactive oxygen species (ROS) (Hue and Taegtmeyer, 2009), and we observed an increase in ROS production in *Srebf1c* KO nerves (Figure 4E) that is likely buffered by a concurrent induction of expression of superoxide dismutase 2 (*Sod2*) and catalase

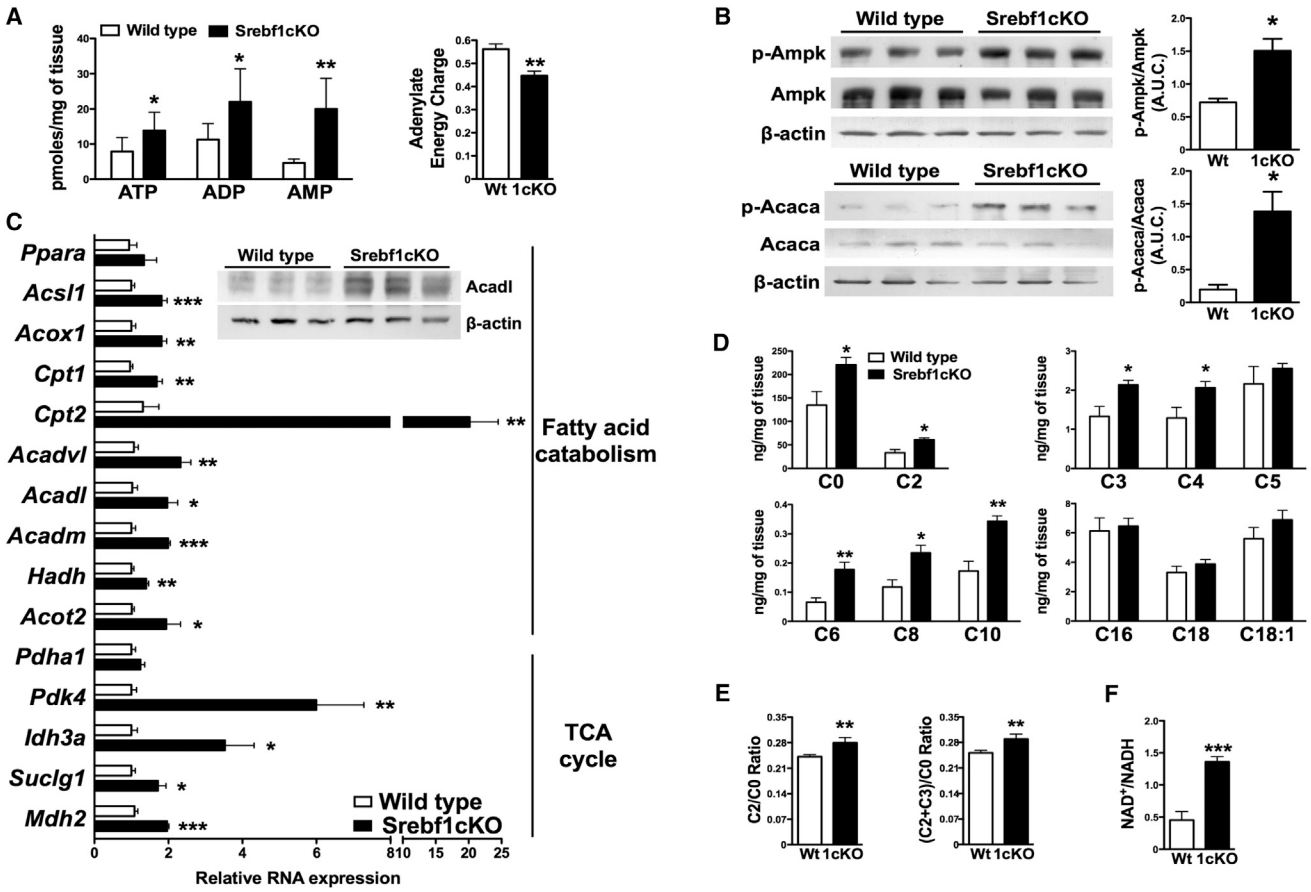

Figure 3. *Srebf1c* KO Sciatic Nerve from 10-Month-Old Mice Displays Energy Depletion and Increased β-Oxidation

(A) Quantification of total ATP, ADP, and AMP levels analyzed by HPLC and adenylate energy charge in sciatic nerve (n = 6 per group).

(B) Western blot analysis and quantification of threonine 172 phosphorylated Ampk, total Ampk, serine 79 phosphorylated Acaca, and total Acaca in sciatic nerve (n = 3 per group).

(C) *Ppara*, *Acsl1*, *Acox1*, *Cpt1*, *Cpt2*, *Acadvl*, *Acadl*, *Acadm*, *Hadh*, *Acot2*, *Pdha1*, *Pdk4*, *Idh3a*, *Suclg1*, and *Mdh2* mRNA and Acadl protein expression in sciatic nerve (n = 6 per group).

(D) Acylcarnitines levels in sciatic nerve (n = 4 per group).

(E) β-oxidation index of even (C2/C0 ratio) and odd (C2 + C3/C0 ratio) FAs in sciatic nerve (n = 4 per group).

(F) NAD^+/NADH ratio in sciatic nerve (n = 3 per group). Data are expressed as mean ± SEM. p values determined by unpaired Student's t test. *p < 0.05, **p < 0.01, and ***p < 0.001 versus wild-type.

(*Cat*) (Figure 4F). The GSH/GSSG ratio was unchanged between wild-type and *Srebf1c* KO nerves (wild-type 0.56 ± 0.01; KO 0.55 ± 0.01; n = 6), excluding generalized oxidative stress in peripheral nerves. Together, these findings demonstrate an increase in FA catabolism and mitochondrial activity in peripheral nerves that results from defects in FA synthesis arising from the lack of *Srebf1c*.

Effects of *Srebf1c* Deficiency on Glucose and Protein Metabolism

In peripheral nerves, a second metabolic pathway affected by the lack of *Srebf1c* was glycolysis (Figures 2A and 2B). 10-month-old *Srebf1c* KO nerves displayed decreased expression of key genes in this pathway such as 6-phosphofructo-2-kinase/fructose 2,6-bisphosphatase isoform 3 (*Pfkfb3*, also known as *Pfk2*), an enzyme involved in the production of activators of phosphofructokinase-1 (*Pfk1*) such as fructose 2,6-bisphosphate (Figure 5A). Moreover, expression of phosphoglycerate kinase 1 (*Pgk1*) was also decreased while hexokinase 1 (*Hk1*) and pyruvate kinase (*Pk*) levels were not affected (Figure 5A). To extend these findings, we measured glucose 6-phosphate and fructose 6-phosphate (as a sum), fructose 1,6-bisphosphate, and pyruvate and lactate as the end products of glycolysis. The levels of glucose 6-phosphate/fructose 6-phosphate were unchanged in *Srebf1c* KO sciatic nerve, indicating that glucose uptake is likely not affected (Figure 5B). On the other hand, the levels of fructose 1,6-bisphosphate, pyruvate, and lactate were reduced in peripheral nerves of *Srebf1c* KO mice (Figure 5B), suggesting that downregulation of *Pfkfb3* expression may be the defective step in the glycolytic pathway of *Srebf1c* KO sciatic nerve. Expression of pyruvate dehydrogenase kinase 4 (*Pdk4*), a negative regulator of the enzyme that converts pyruvate from glycolysis into acetyl-CoA (pyruvate dehydrogenase alpha 1, *Pdha1*), was increased in *Srebf1c* KO

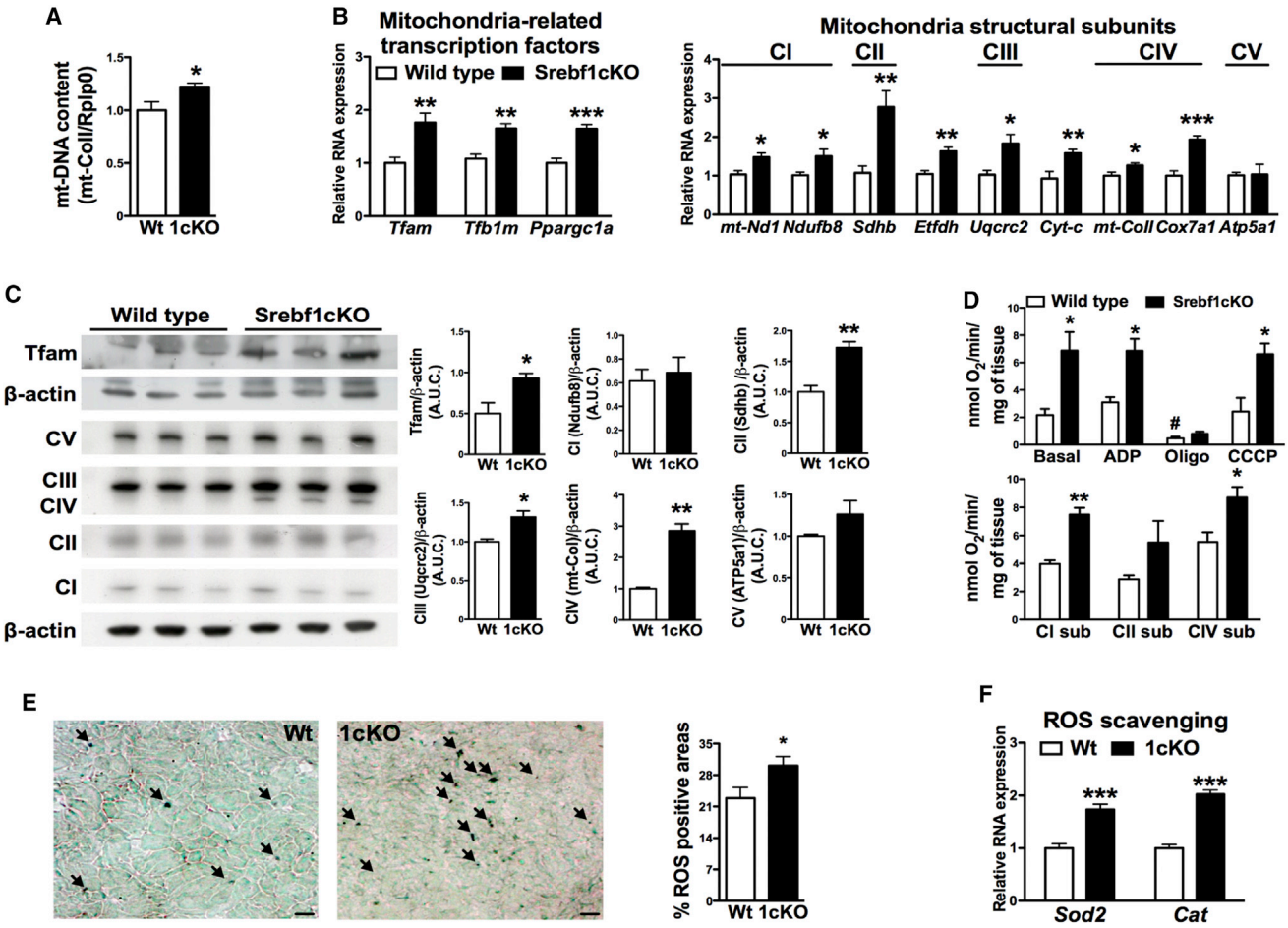

Figure 4. Mitochondrial Function Is Increased in the Sciatic Nerve of 10-Month-Old *Srebf1c* KO Mice

(A) Mitochondrial DNA content of sciatic nerve (n = 5 per group).

(B) qRT-PCR analysis of *Tfam*, *Tfb1m*, *Ppargc1a*, *mt-Nd1*, *Ndufb8*, *Sdhb*, *Etfdh*, *Uqcrc2*, *Cyt-c*, *mt-CoII*, *Cox7a1*, and *Atp5a1* (n = 6 per group).

(C) Western blot analysis of Tfam and indicated ETC subunits in sciatic nerve and relative quantification (n = 3 per group).

(D) Mitochondrial respiration and ETC complexes activity (n = 3 per group).

(E) Histochemical analysis of ROS production and relative quantification (n = 7 per group). Scale bar, 10 μm.

(F) Expression of *Sod2* and *Cat* mRNA (n = 6 per group). Data are expressed as mean ± SEM. p values determined by unpaired Student's t test. *$p < 0.05$, **$p < 0.01$, and ***$p < 0.001$ versus wild-type; $^{\#}p < 0.05$ versus basal wild-type.

nerves, which suggests reduced flux of pyruvate into the TCA cycle (Figure 3C). The levels of pyruvate and lactate were unchanged in *Srebf1c* KO liver (Figure S4D), but expression of glucokinase (*Gck*), a direct target of Srebf1c, was decreased as has been previously reported (Liang et al., 2002) (Figure S3B).

Peripheral neuropathies have been linked to perturbations in endoplasmic reticulum (ER) homeostasis that engage the UPR (D'Antonio et al., 2013; Viader et al., 2013). The gene expression profile of major players in the UPR and the phosphorylation status of eukaryotic translation initiation factor 2a (Eif2a), a regulator of protein translation in the context of UPR, were not significantly altered in *Srebf1c* KO peripheral nerves (Figures 5C and 5D). However, expression of genes associated with ER quality control systems such as unfolded protein binding, ER protein folding, ER-associated degradation (ERAD), and ubiquitination was significantly increased in *Srebf1c* KO nerves (Figure 5E). This protein-proofreading pathway controls the native conformation of proteins such that properly folded proteins are transported to their final destination while unfolded or misfolded proteins are ubiquitinated and degraded (Ellgaard and Helenius, 2003). The pattern of total protein ubiquitination was significantly greater in *Srebf1c* KO peripheral nerves (Figure 5F), and the amino acid profile of *Srebf1c* KO sciatic nerve showed a general increase in these metabolites consistent with a higher rate of proteolysis (Figure S5A). These alterations were specific to peripheral nerves, for liver and plasma from *Srebf1c* KO mice did not display this pattern (Figures S5B and S5C). Furthermore, expression of liver UPR (Figure S3B) and ER quality control genes was not increased (data not shown). These data suggest that reduced glucose oxidation in *Srebf1c* KO peripheral nerves boosts expression of ER quality control genes and augments general protein ubiquitination and degradation.

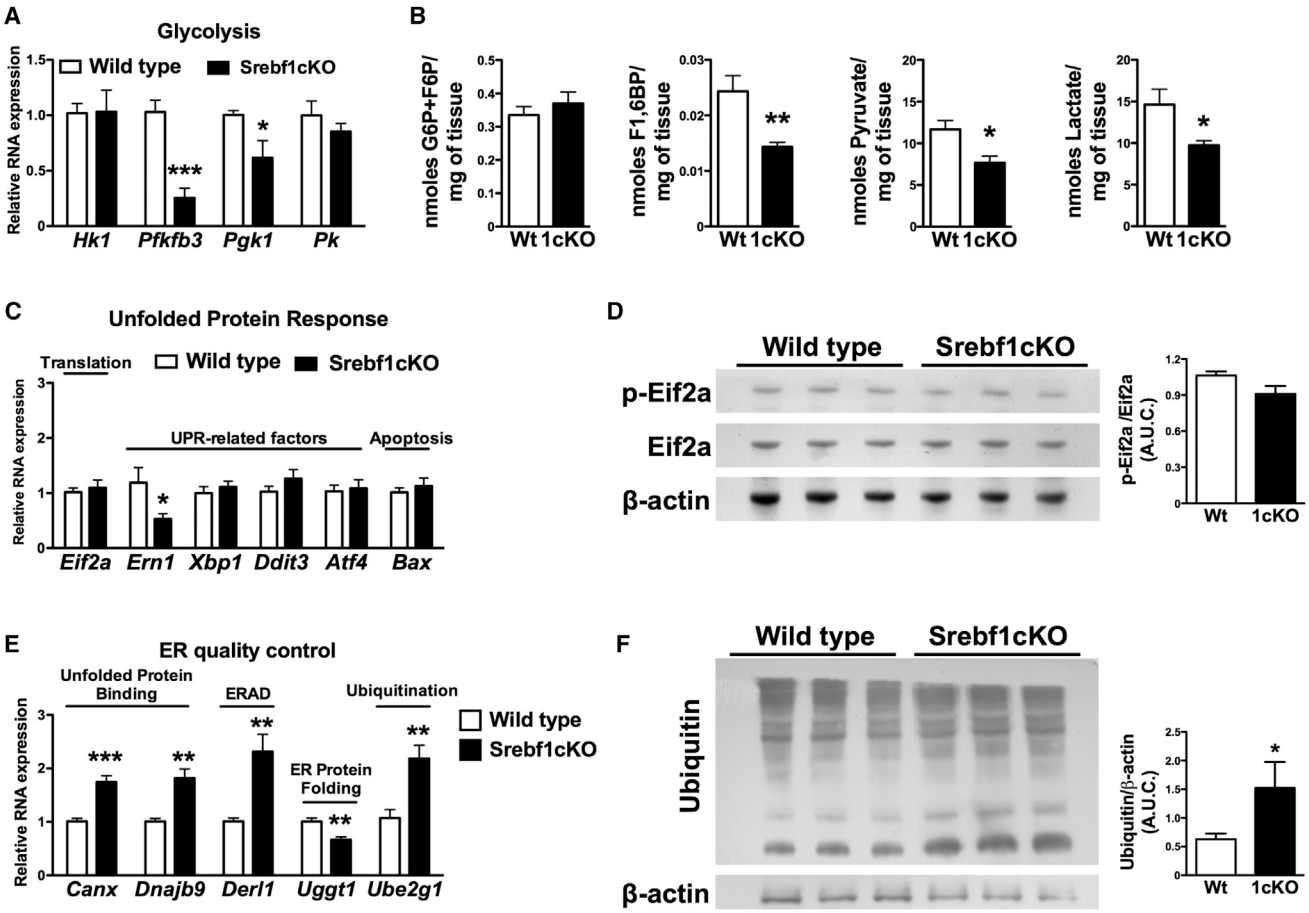

Figure 5. The Sciatic Nerve of 10-Month-Old *Srebf1c* KO Mice Shows Reduced Glycolysis and Induction of the ER Quality Control System

(A) qRT-PCR analysis of *Hk1*, *Pfkfb3*, *Pgk1*, and *Pk* expression (n = 6 per group).

(B) Levels of glucose 6-phosphate/fructose 6-phospate, fructose 1,6-bisphosphate, pyruvate, and lactate in sciatic nerve (n = 6 per group).

(C and D) (C) mRNA expression levels of *Eif2a*, *Ern1*, *Xbp1*, *Ddit3*, *Atf4*, *and Bax* (n = 6 per group), and (D) western blot analysis of serine 51 phosphorylated Eif2a and total Eif2a and quantification (n = 3 per group).

(E and F) (E) Gene expression analysis of *Canx*, *Dnajb9*, *Uggt1*, *Derl1*, and *Ube2g1* (n = 6 per group), and (F) western blot analysis of global protein ubiquitination and its quantification (n = 3 per group). Data are expressed as mean ± SEM. p values determined by unpaired Student's t test. *p < 0.05, **p < 0.01, and ***p < 0.001 versus wild-type.

Activation of Pparα Specifically in Schwann Cells Drives Development of Peripheral Neuropathy

To investigate the molecular basis of the metabolic changes that characterize peripheral neuropathy development in *Srebf1c* KO peripheral nerves, we next explored the extent to which absence of *Srebf1c* results in aberrant Pparα signaling. Pparα is a ligand-activated transcription factor that is a primary regulator of FA catabolism (Bantubungi et al., 2012; Kersten et al., 1999). Endogenous Pparα ligands include lipids in the phosphatidylcholine (PC) family, specifically PC-C16:0/C18:1 and PC-C18:0/C18:1 (Chakravarthy et al., 2009; Liu et al., 2013). Using targeted metabolomics, 88 different glycerophospholipids (GPLs) and 14 sphingolipids (SLs) were profiled in sciatic nerves from 10-month-old *Srebf1c* KO and wild-type mice (Figure S5E). *Z* score analysis of GPL and SL species statistically different between genotypes indicated that the most abundant species in *Srebf1c* KO sciatic nerve were PC aa C34:1 and PC aa C36:1 (Figure 6A). Tandem mass spectrometry identified PC aa C34:1 as PC-C16:0/C18:1 and PC aa C36:1 as PC-C18:0/C18:1 (Figures S6A and S6B). The levels of both of these species were increased in *Srebf1c* KO peripheral nerves (Figure 6B). Analysis of GPL and SL species in liver and plasma yielded a different profile of changes in *Srebf1c* KO samples (Figures S4B and S7A). Interestingly, the levels PC aa C34:1 and PC aa 36:1 in *Srebf1c* KO livers were unchanged while those in plasma were decreased (Figures S4C and S7B).

To investigate the functional consequences of these metabolome changes, we first confirmed that the level of *Pparα* expression was not different between *Srebf1c* KO and wild-type nerves (Figure 3C), and that Pparα-mediated transcription could be activated by PC-C16:0/C18:1 and PC-C18:0/C18:1 in a cell-based assay (Figure S5D). We then used chromatin immunoprecipitation (ChIP) assays in sciatic nerves to evaluate the level of Pparα activity in situ. ChIP analysis of 10-month-old peripheral nerves revealed greater enrichment of Pparα bound to its responsive elements (PPRE) within the promoter of both acyl-CoA oxidase

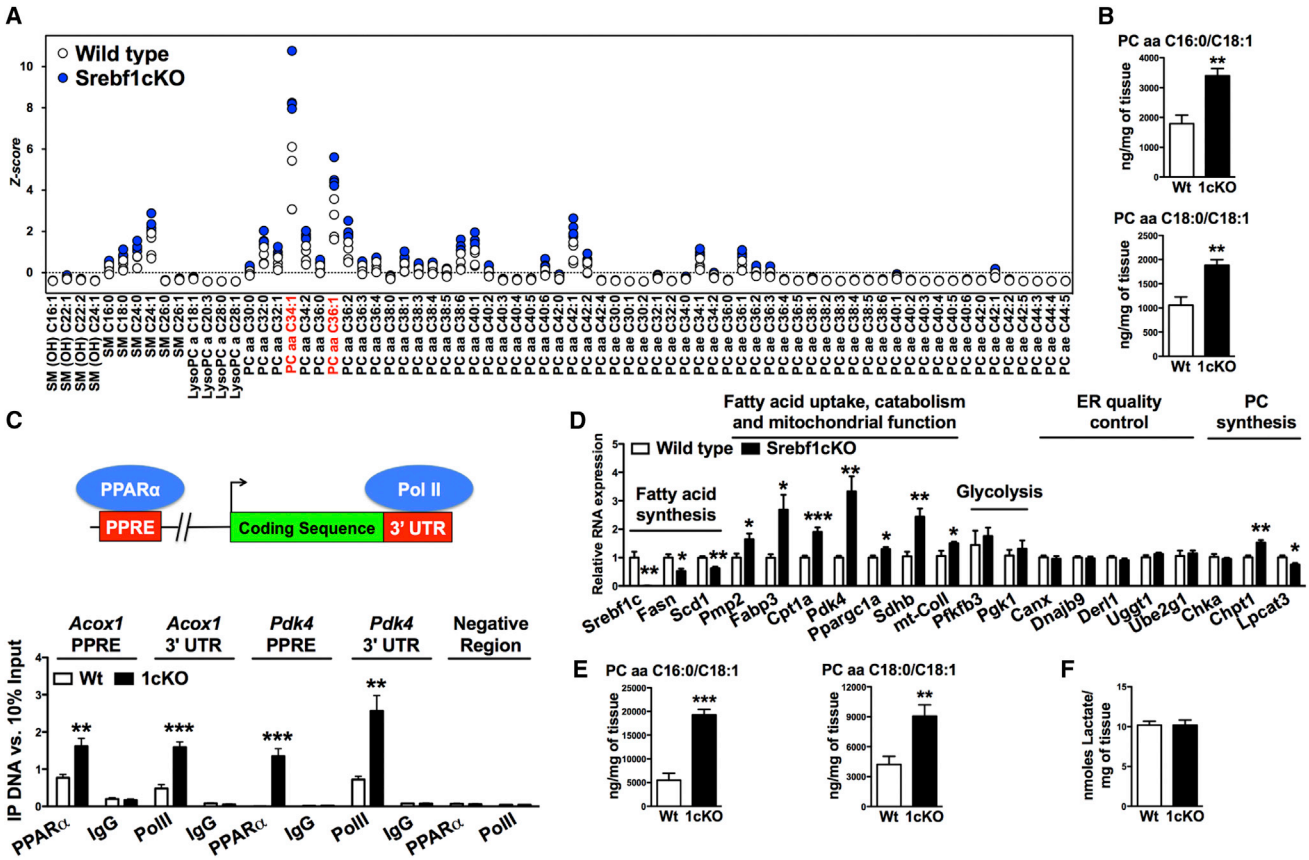

Figure 6. PC aa C16:0/C18:1 and PC aa C18:0/C18:1 Activate Pparα in *Srebf1c* KO Nerve

(A) *Z* score of significantly altered GPL and SL species levels in 10-month-old *Srebf1c* KO sciatic nerve relative to wild-type.

(B) PC aa C16:0/C18:1 and PC aa C18:0/C18:1 quantification (n = 4 per group).

(C) ChIP analysis of Pparα recruitment to Pparα responsive elements (PPRE), and of active Pol II within the *Acox1* and *Pdk4* promoters and 3′ UTRs, respectively, in sciatic nerves of 10-month-old mice (n = 6 per group).

(D) qRT-PCR analysis of *Srebf1c*, *Fasn*, *Scd1*, *Pmp2*, *Fabp3*, *Cpt1a*, *Pdk4*, *Ppargc1a*, *Sdhb*, *mt-CoII*, *Pfkfb3*, *Pgk1*, *Canx*, *Dnajb9*, *Derl1*, *Uggt1*, *Ube2g1*, *Chka*, *Chpt1*, and *Lpcat3* in sciatic nerve of 2-month-old mice (n = 5 per group).

(E) PC aa C16:0/C18:1 and PC aa C18:0/C18:1 levels in sciatic nerves at 2 months of age (n = 5 per group).

(F) Lactate levels in sciatic nerve of 2-month-old mice (n = 5 per group). Data are expressed as mean ± SEM. p values determined by unpaired Student's t test. *p < 0.05, **p < 0.01, and ***p < 0.001 versus wild-type.

1 (*Acox1*) and *Pdk4* genes (Figure 6C) in *Srebf1c* KO nerves. We also detected increased amounts of polymerase II (*Pol II*) at the 3′ UTR of both *Acox1* and *Pdk4* genes in *Srebf1c* KO peripheral nerves, a strong indication that this greater level of Pparα recruitment translates into an enhanced level of target gene expression (Figure 6C). These ChIP data are supported by our original RT-qPCR analysis that shows increased expression of *Acox1* and *Pdk4* in *Srebf1c* KO peripheral nerves (Figure 3C).

To examine if our findings in *Srebf1c* KO peripheral nerves could be ascribed primarily to either the glial or the neuronal compartment, we used transcriptomics and metabolomics to profile DRG from 10-month-old mice. Remarkably, despite reduced expression of FA synthesis genes in *Srebf1c* KO DRG, the level of expression of FA catabolism genes was not different between genotypes (Figure S7C). More importantly, neither the C2/C0 and C2+C3/C0 ratios nor the levels of PC-C16:0/C18:1 and PC-C18:0/C18:1 were altered in *Srebf1c* KO DRG (Figures S7D and S7E). These findings indicate that absence of *Srebf1c* and the consequent reduction in FA synthesis primarily affects Schwann cell physiology to bring about the observed glial abnormalities.

Our observations in 10-month-old *Srebf1c* KO mice with well-established peripheral neuropathy indicate that a metabolic shift from glucose toward FA oxidation and altered ER quality control are both present. Since either of these abnormalities could in principle result in peripheral neuropathy, to discern which of these aberrations may be the primary driver in disease development we studied the peripheral nerves of 2-month-old wild-type and *Srebf1c* KO mice. Because at this age *Srebf1c* KO mice exhibit a significantly milder neuropathic phenotype, they are likely to be more informative regarding the causal alteration that drives defects in nerve structure and function in older animals. Gene expression analysis detected significant upregulation of genes involved in FA uptake, transport, and catabolism, as well as mitochondrial function in the sciatic nerve of 2-month-old *Srebf1c* KO mice (Figure 6D), suggesting increased

Pparα activity. Consistent with this notion, the levels of the endogenous Pparα ligands PC-C16:0/C18:1 and PC-C18:0/C18:1 were increased in *Srebf1c* KO peripheral nerves at this early age (Figure 6E). Importantly, the expression of choline phosphotransferase 1 (*Chpt1*), an enzyme of the PC biosynthetic pathway, was increased (Figure 6D). In contrast, the expression of lysophosphatidylcholine acyltransferase 3 (*Lpcat3*) was reduced (Figure 6D). Lpcat3 is a remodeling enzyme that preferentially uses polyunsaturated fatty acyl-CoAs as donors for lyso-PC substrates (Lands, 1958). Because a decrease in Lpcat3 activity is expected to shift incorporation into lyso-PC from polyunsaturated to monounsaturated or saturated FAs, it is likely that this defect results in the increased levels of PC-C16:0/C18:1 and PC-C18:0/C18:1 measured in *Srebf1c* KO nerves. In contrast to these metabolic differences indicative of induction of Pparα signaling, we did not detect alterations in glycolysis or ER quality control in 2-month-old *Srebf1c* KO nerves (Figures 6D and 6F), suggesting that it is the induction of Pparα activity that drives the development of peripheral neuropathy in these animals. Interestingly, the changes in gene expression of key genes in FA catabolism, glycolysis, and mitochondrial function seen in vivo were recapitulated in the mouse Schwann cell line MSC80 treated with either PC-C16:0/C18:1 or PC-C18:0/C18:1 (Figure S7F).

Inhibition of Pparα Activity Ameliorates Peripheral Neuropathy in *Srebf1c* KO Mice

To examine if inhibition of Pparα would reverse the neuropathic phenotype, 10-month-old *Srebf1c* KO mice were treated either with vehicle or the Pparα antagonist GW6471 (Xu et al., 2002) for 15 days. Using ChIP assays we found that GW6471 treatment induced in *Srebf1c* KO sciatic nerves recruitment of the transcriptional corepressor NCoR to the PPRE of *Acox1* and *Pdk4*, indicating that the antagonist reached the sciatic nerve and acted to block Pparα function (Figure 7D). As consequence of GW6471 treatment, the functional (Figures 7A and 7B), morphological (Figure 7C), gene expression (Figure 7E), and acylcarnitine level (Figure 7F) abnormalities present in 10-month-old *Srebf1c* KO nerves were reversed to those of peripheral neuropathy-free wild-type mice. These data indicate that inhibition of anomalous Pparα activation can rescue the neuropathic phenotype seen in *Srebf1c* KO mice. Finally, to explore if the opposite would also be true, wild-type mice were treated with either vehicle or two different Pparα agonists (Wy14643 and fenofibrate) for 15 days. Treatment with these synthetic Pparα activators increased Pparα target gene expression and induced FA oxidation in sciatic nerve (Figures 7I and 7J) and had a negative impact on nerve functional parameters (thermal and mechanical nociceptive thresholds Figures 7G and 7H), mimicking several features of the neuropathic phenotype observed in *Srebf1c* KO mice. Taken together, these results demonstrate that aberrant activation of Pparα signaling in *Srebf1c* KO nerves induces a metabolic shift toward FA oxidation that ultimately results in the development of peripheral neuropathy.

DISCUSSION

Genetic models have demonstrated that alterations in cholesterol (Saher et al., 2009) and lipid (Verheijen et al., 2009) metabolism, or peroxisomal FA catabolism (Kassmann et al., 2007; Van Veldhoven, 2010; Wierzbicki et al., 2002) can result in peripheral myelin abnormalities and/or peripheral neuropathy, but less is known about the impact of endogenous FA biosynthesis on peripheral nerve integrity and function. The glial component of the peripheral nervous system requires massive amounts of FAs to properly myelinate peripheral nerves (Garbay et al., 2000). Schwann cells fulfill this requirement by synthesizing FAs and by taking up FAs from the bloodstream and from other nerve structures (Bourre et al., 1987; Verheijen et al., 2003, 2009; Yao et al., 1980). To directly evaluate the relevance of endogenous FA synthesis on peripheral nerve structure and function, here we studied a mouse model of blunted FA synthesis (Liang et al., 2002), the *Srebf1c* KO. We have found that lack of the lipogenic transcription factor *Srebf1c* is sufficient to bring about peripheral neuropathy.

Peripheral neuropathy in *Srebf1c* KO mice is characterized by altered functional, morphological, and morphometric parameters. Due to altered myelin periodicity, 10-month-old *Srebf1c* KO mice have hypermyelinated small-caliber fibers that appear expanded and yield myelin instability, as shown by the decrease in NCV measured in these mice. In addition, we also observed subtle effects on Remak bundles, suggesting that reduced FA synthesis affects both myelinating and non-myelinating Schwann cells. Transcriptomic and metabolomic analyses in 10-month-old mice revealed that lack of *Srebf1c* induced a shift from FA synthesis toward catabolism specifically in peripheral nerves. These data are consistent with findings in KO models of FA biosynthetic enzymes that show increased liver FA catabolism when fed either chow or high-carbohydrate or -fat diets (Strable and Ntambi, 2010). However, in the fed state, *Srebf1c* KO livers did not display increased oxidative metabolism, and our observations in the sciatic nerve were restricted to this tissue. Moreover, the increase in FA catabolism appears to be Schwann cell specific, as we found no induction of this pathway in DRG or in plasma.

The mechanism responsible for enhanced FA catabolism in *Srebf1c* KO mice restricted to peripheral nerves appears to be the accumulation of PC-C16:0/C18:1 and PC-C18:0/C18:1 specifically in the sciatic nerve. Increased levels of these two endogenous Pparα ligands activate this transcription factor in vivo primarily in Schwann cells, resulting in increased FA catabolism and the eventual development of peripheral neuropathy (Figure 7K). This model is supported by the energy depletion measured in *Srebf1c* KO nerves that resulted in Ampk activation and the subsequent inhibition of Acaca, thus shifting FA flux toward β-oxidation in *Srebf1c* KO nerves. Importantly, treatment of 10-month-old *Srebf1c* KO mice with a Pparα antagonist reversed the functional nerve deficits associated with peripheral neuropathy, indicating that aberrant activation of Pparα-mediated transcription is indeed the main driver of peripheral neuropathy in these mice.

Although they showed no defect in glucose uptake, 10-month-old *Srebf1c* KO nerves also displayed deficiencies in glycolytic gene expression. As a consequence, the levels of fructose 1,6-bisphosphate, pyruvate, and lactate were all decreased, indicating that *Srebf1c* KO peripheral nerves had shifted from glycolytic to oxidative metabolism. These results are noteworthy considering that peripheral nerves rely on glucose and lactate to

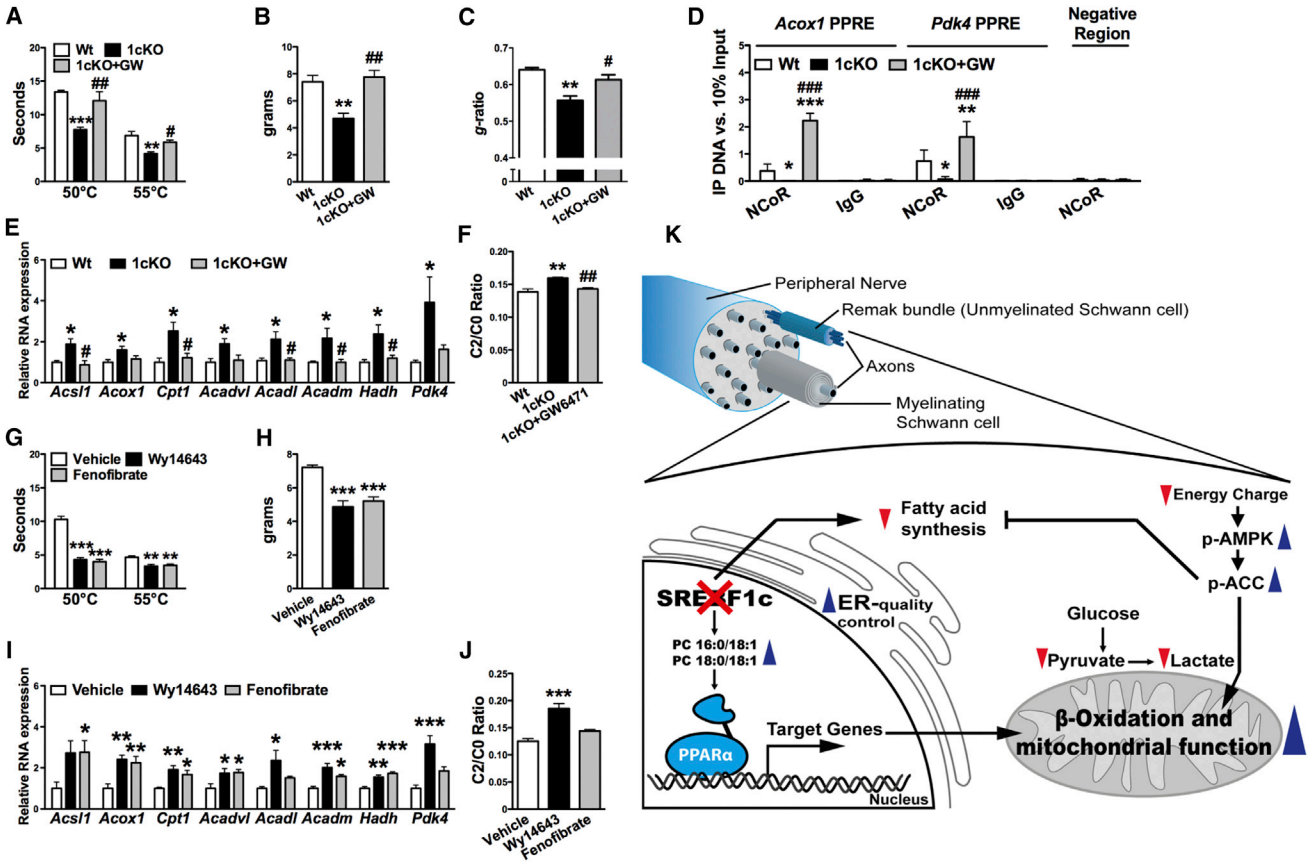

Figure 7. Aberrant Pparα Signaling Drives Development of Peripheral Neuropathy in *Srebf1c* KO Mice

(A and B) Thermal and mechanical nociceptive threshold in 10-month-old mice treated either with vehicle or the Pparα antagonist GW6471 (n = 6 per group).

(C) *g* ratio of sciatic nerve small-caliber myelinated fibers (<4 μm) from mice in (A) and (B) (n = 3 per group).

(D) ChIP analysis of NCoR recruitment to Pparα responsive elements (PPREs) within the *Acox1* and *Pdk4* promoters from mice shown in (A) and (B) (n = 6 per group).

(E) Expression of *Acsl1*, *Acox1*, *Cpt1*, *Acadvl*, *Acadl*, *Acadm*, *Hadh*, and *Pdk4* mRNA in mice shown in (A) and (B) (n = 6 per group).

(F) β-oxidation index of even FAs in sciatic nerve of mice shown in (A) and (B) (n = 6 per group).

(G and H) Thermal and mechanical nociceptive threshold in wild-type mice (2 months old) treated with vehicle, Wy14643, or fenofibrate (n = 5 per group).

(I) Expression of *Acsl1*, *Acox1*, *Cpt1*, *Acadvl*, *Acadl*, *Acadm*, *Hadh*, and *Pdk4* mRNA in sciatic nerve mice shown in (G) and (H) (n = 5 per group).

(J) Sciatic nerve β-oxidation index of even FAs in wild-type mice shown in (G) and (H) (n = 5 per group).

(K) Schematic representation of the putative molecular mechanism underlying neuropathy development in *Srebf1c* KO sciatic nerves. Data are expressed as mean ± SEM. p values for three-group comparisons determined by one-way ANOVA followed by Tukey's multiple comparison post hoc test. $^{*}p < 0.05$, $^{**}p < 0.01$, and $^{***}p < 0.001$ versus wild-type or vehicle; $^{\#}p < 0.05$, $^{\#\#}p < 0.01$, and $^{\#\#\#}p < 0.001$ versus *Srebf1c* KO.

maintain their function (Beirowski, 2013). Moreover, because ensheathing cells such as Schwann cells in the peripheral nervous system provide metabolic support to fulfill the energy demand of sustained axonal functions (Nave, 2010; Nave and Trapp, 2008), the glycolytic deficiencies of *Srebf1c* KO Schwann cells could negatively impact nerve function. Defects in glycolysis were also accompanied by derangements in the ER quality control system in *Srebf1c* KO sciatic nerves, as indicated by increased protein ubiquitination and proteolysis.

Although we observed these abnormalities in glycolysis and ER quality control in 10-month-old *Srebf1c* KO nerves, study of younger mice with a milder neuropathy showed that the primary defect that drives development of peripheral neuropathy in *Srebf1c* KO mice is a shift toward FA oxidation. Metabolome and transcriptome profiles of peripheral nerves in these younger mice revealed increased levels of PC-C16:0/C18:1 and PC-C18:0/C18:1 that are the result of induced PC synthesis as well as altered PC remodeling and availability of local FAs, but no defects in glycolysis or ER quality control.

Our findings suggest that Pparα activation plays a critical role in the pathogenesis of peripheral neuropathy development, at least in certain settings. *Srebf1c* KO mice displayed mechanical and thermal hyperalgesia at both 2 and 10 months of age along with increased levels of endogenous Pparα ligands and augmented FA catabolism in peripheral nerves. Furthermore, wild-type mice treated with synthetic Pparα agonists phenocopied several aspects of the *Srebf1c* KO neuropathic phenotype. It is tempting to suggest that these data provide a partial explanation for the sporadic cases of peripheral neuropathy that have been reported in humans treated with fibrates (Corcia et al., 1999; Corrao et al., 2004; Gabriel and Pearce, 1976). However, several studies have also demonstrated a beneficial effect of

Pparα agonists in a variety of animal pain models, including ligation of the sciatic nerve to induce mechanical and thermal hyperalgesia (Fehrenbacher et al., 2009; LoVerme et al., 2006). This discrepancy is likely due to the anti-inflammatory effects of Pparα activation in those models (LoVerme et al., 2006), effects that are not seen in *Srebf1c* KO sciatic nerves.

In summary, our work reveals that lack of *Srebf1c* results in defects in FA synthesis and glycolysis that unexpectedly force Schwann cells to rely on FAs as a fuel source and that FA catabolism in these cells is driven by the accumulation of endogenous activators of Pparα, a critical regulator of FA catabolism. These data provide new insight into the contribution of endogenous FA synthesis to nerve homeostasis and function that when impaired can lead to the development of peripheral neuropathy.

EXPERIMENTAL PROCEDURES

Animals

Srebf1c heterozygous null mice were purchased from The Jackson Laboratory (B6;129S6-*Srebf1*^{tm1Jdh}, stock number: 004365) and used to generate a colony of homozygous *Srebf1c* KO animals. C57BL6/J were purchased from Charles River. All experiments were conducted following the regulations of the European Community (Directive 86/609/EEC, Official Journal L 358, 18/12/1986 p. 0001-0028) and local regulations (e.g., Italian Legislative Decree n. 116 - 27/01/1992) for the care and use of laboratory animals. The Italian Ministry of Health approved the animal protocols of this study (ministerial decree n. 295/2012-A).

Peripheral Neuropathy Assessment

All behavioral tests used to evaluate the degree of peripheral neuropathy were performed in a blind fashion.

Thermal Nociceptive Threshold

Nociceptive threshold to radiant heat was quantified using the hot plate paw withdrawal test. The test was carried out at both 50°C ± 0.2°C and 55°C ± 0.2°C.

Mechanical Nociceptive Threshold

The dynamic test was used to assess the development of mechanical allodynia in wild-type versus *Srebf1c* KO animals. The dynamic aesthesiometer test (Ugo Basile) was calibrated to exert a progressively increasing punctate pressure with a gram force ramp of 1 g/s. After a clear hind paw withdrawal, the instrument automatically stopped the stimulus, and the gram force obtain indicated the mechanical nociceptive threshold index.

NCV

Digital NCV and nerve action potential amplitudes were measured using an electromyography apparatus (Myto2 ABN Neuro) to assess the sensory/motor functional status, as previously described (Carozzi et al., 2013).

IENF Density

Peripheral nerve damage was assessed by the quantification of the IENF density in the skin of the hindpaw footpad collected at sacrifice (Lauria et al., 2005).

Morphometric Analysis and Transmission Electron Microscopy of Myelin

Freshly isolated sciatic nerves from wild-type and *Srebf1c* KO mice were cut in segments (1 to 2 mm length) and fixed. Samples were postfixed in 1% buffered OsO_4, dehydrated in an acetone gradient and embedded in TAAB low-viscosity resin. Myelinated fibers were stained with toluidine blue. The number of fibers per nerve, the *g*-ratio, the percentage of fibers with infoldings, the number of altered axons in Remak bundles, and myelin periodicity were analyzed in ultrathin sections using a JEOL 1200 EXII electron microscope. The *g* ratio was calculated as the quotient between the axon size and the fiber size.

Gene Expression and Microarray Analysis

RNA from sciatic nerve, DRG, and liver of wild-type and *Srebf1c* KO mice was isolated with TRIzol (Invitrogen) and purified using the Nucleospin RNA II kit (Macherey-Nagel). Samples were quantified by real-time PCR using SYBR Green or TaqMan probes on a CFX384 real time system using the iScriptTM one-step qRT-PCR kit for SYBR Green or for probes (Bio-Rad Laboratories). Target gene expression was normalized to 36B4. Primers and probes are available upon request. For microarray experiments, RNA was analyzed by the Genopolis Consortium using an Affimetrix platform (GEO accession number GSE65754). Gene Ontology biological process analysis was performed using Panther software (http://www.pantherdb.org/).

Metabolomic Analyses

For metabolomic analyses, sciatic nerves, DRG, and liver were homogenized in methanol with a tissue lyser. Aliquots of plasma and/or of methanolic extracts were directly processed according to the manufacturer's instructions (AbsoluteIDQ p180 Kit, Biocrates). Quantitative analysis of FAs was performed as previously described (Cermenati et al., 2012).

Mitochondrial Respiration and ROS Production

All assays were performed with a DW1 Electrode Chamber (Hansatech Instruments Ltd), and data were normalized to tissue weight. Respiration assays were evaluated as previously reported (Rogers et al., 2011). ROS were evaluated on 10 μm cryostat sections of sciatic nerves as described by Kerver et al. (1997).

Statistical Analysis

Statistical analyses were performed by Student's t test for the comparison of two different experimental groups, or one-way ANOVA with the indicated post hoc test for multiple testing comparisons. All statistical analyses were performed using GraphPad Prism (GraphPad Software).

SUPPLEMENTAL INFORMATION

Supplemental Information includes seven figures and Supplemental Experimental Procedures and can be found with this article online at http://dx.doi.org/10.1016/j.cmet.2015.02.016.

AUTHOR CONTRIBUTIONS

G. Cermenati and M.A. designed and performed experiments, interpreted results, and wrote the manuscript. S.G., V.C., C.P.-S., and G. Cavaletti performed functional tests. E.P., C.F., M.D., I.A., and L.M.G.S. performed morphological/morphometric studies and interpreted results. S.S. performed metabolomics. E.S., E.D.F., and M.C. analyzed data, interpreted results, and wrote the manuscript. R.C.M., D.C., and N.M. designed experiments, analyzed data, and wrote the manuscript.

ACKNOWLEDGMENTS

We thank F. Giavarini for his valuable help with HPLC and mass spectrometry and M.I. Maher and M.C. Panzeri for technical assistance with electron microscopy. We also thank F. Gardoni, G. Lauria, S. Ghisletti, A. Galmozzi, and V. Lo Sardo for critically reading the manuscript and for their helpful comments. We are in debt with Ms. E. Desiderio Pinto for administrative assistance. These studies were supported by funding from Giovanni Armenise-Harvard Foundation Career Development Grant (N.M.), Fondazione CARIPLO 2014-0991 (N.M.), Fondazione CARIPLO 2012-0547 (R.C.M.), Italian Ministry of Health GR-2011-02346791 (M.D. and N.M.) and Research Center for the Characterization and Safe Use of Natural Compounds—"Giovanni Galli" directed by D.C. S.S. is an employee and founder of DASP s.r.l.; all other authors declare no competing financial interests.

Received: July 14, 2014
Revised: January 9, 2015
Accepted: February 19, 2015
Published: March 26, 2015

REFERENCES

Atkinson, D.E., and Walton, G.M. (1967). Adenosine triphosphate conservation in metabolic regulation. Rat liver citrate cleavage enzyme. J. Biol. Chem. *242*, 3239–3241.

Bantubungi, K., Prawitt, J., and Staels, B. (2012). Control of metabolism by nutrient-regulated nuclear receptors acting in the brain. J. Steroid Biochem. Mol. Biol. *130*, 126–137.

Beirowski, B. (2013). Concepts for regulation of axon integrity by enwrapping glia. Front. Cell Neurosci. *19*, 256.

Bourre, J.M., Youyou, A., Durand, G., and Pascal, G. (1987). Slow recovery of the fatty acid composition of sciatic nerve in rats fed a diet initially low in n-3 fatty acids. Lipids *22*, 535–538.

Carozzi, V.A., Renn, C.L., Bardini, M., Fazio, G., Chiorazzi, A., Meregalli, C., Oggioni, N., Shanks, K., Quartu, M., Serra, M.P., et al. (2013). Bortezomib-induced painful peripheral neuropathy: an electrophysiological, behavioral, morphological and mechanistic study in the mouse. PLoS ONE *8*, e72995.

Cermenati, G., Abbiati, F., Cermenati, S., Brioschi, E., Volonterio, A., Cavaletti, G., Saez, E., De Fabiani, E., Crestani, M., Garcia-Segura, L.M., et al. (2012). Diabetes-induced myelin abnormalities are associated with an altered lipid pattern: protective effects of LXR activation. J. Lipid Res. *53*, 300–310.

Chakravarthy, M.V., Lodhi, I.J., Yin, L., Malapaka, R.R., Xu, H.E., Turk, J., and Semenkovich, C.F. (2009). Identification of a physiologically relevant endogenous ligand for PPARalpha in liver. Cell *138*, 476–488.

Corcia, P., de Toffol, B., Hommet, C., Autret, A., and Jonville-Bera, A.P. (1999). Severe toxic neuropathy due to fibrates. J. Neurol. Neurosurg. Psychiatry *66*, 410.

Corrao, G., Zambon, A., Bertù, L., Botteri, E., Leoni, O., and Contiero, P. (2004). Lipid lowering drugs prescription and the risk of peripheral neuropathy: an exploratory case-control study using automated databases. J. Epidemiol. Community Health *58*, 1047–1051.

Correa-Cerro, L.S., Wassif, C.A., Kratz, L., Miller, G.F., Munasinghe, J.P., Grinberg, A., Fliesler, S.J., and Porter, F.D. (2006). Development and characterization of a hypomorphic Smith-Lemli-Opitz syndrome mouse model and efficacy of simvastatin therapy. Hum. Mol. Genet. *15*, 839–851.

D'Antonio, M., Musner, N., Scapin, C., Ungaro, D., Del Carro, U., Ron, D., Feltri, M.L., and Wrabetz, L. (2013). Resetting translational homeostasis restores myelination in Charcot-Marie-Tooth disease type 1B mice. J. Exp. Med. *210*, 821–838.

de Preux, A.S., Goosen, K., Zhang, W., Sima, A.A., Shimano, H., Ouwens, D.M., Diamant, M., Hillebrands, J.L., Rozing, J., Lemke, G., et al. (2007). SREBP-1c expression in Schwann cells is affected by diabetes and nutritional status. Mol. Cell. Neurosci. *35*, 525–534.

Ellgaard, L., and Helenius, A. (2003). Quality control in the endoplasmic reticulum. Nat. Rev. Mol. Cell Biol. *4*, 181–191.

Fehrenbacher, J.C., Loverme, J., Clarke, W., Hargreaves, K.M., Piomelli, D., and Taylor, B.K. (2009). Rapid pain modulation with nuclear receptor ligands. Brain Res. Brain Res. Rev. *60*, 114–124.

Fitzky, B.U., Moebius, F.F., Asaoka, H., Waage-Baudet, H., Xu, L., Xu, G., Maeda, N., Kluckman, K., Hiller, S., Yu, H., et al. (2001). 7-Dehydrocholesterol-dependent proteolysis of HMG-CoA reductase suppresses sterol biosynthesis in a mouse model of Smith-Lemli-Opitz/RSH syndrome. J. Clin. Invest. *108*, 905–915.

Gabriel, R., and Pearce, J.M. (1976). Clofibrate-induced myopathy and neuropathy. Lancet *2*, 906.

Garbay, B., Heape, A.M., Sargueil, F., and Cassagne, C. (2000). Myelin synthesis in the peripheral nervous system. Prog. Neurobiol. *61*, 267–304.

Hardie, D.G., Ross, F.A., and Hawley, S.A. (2012). AMPK: a nutrient and energy sensor that maintains energy homeostasis. Nat. Rev. Mol. Cell Biol. *13*, 251–262.

Horton, J.D., Goldstein, J.L., and Brown, M.S. (2002). SREBPs: activators of the complete program of cholesterol and fatty acid synthesis in the liver. J. Clin. Invest. *109*, 1125–1131.

Hue, L., and Taegtmeyer, H. (2009). The Randle cycle revisited: a new head for an old hat. Am. J. Physiol. Endocrinol. Metab. *297*, E578–E591.

Hughes, R.A. (2002). Peripheral neuropathy. BMJ *324*, 466–469.

Kassmann, C.M., Lappe-Siefke, C., Baes, M., Brügger, B., Mildner, A., Werner, H.B., Natt, O., Michaelis, T., Prinz, M., Frahm, J., and Nave, K.A. (2007). Axonal loss and neuroinflammation caused by peroxisome-deficient oligodendrocytes. Nat. Genet. *39*, 969–976.

Kennedy, W.R., Wendelschafer-Crabb, G., and Johnson, T. (1996). Quantitation of epidermal nerves in diabetic neuropathy. Neurology *47*, 1042–1048.

Kersten, S., Seydoux, J., Peters, J.M., Gonzalez, F.J., Desvergne, B., and Wahli, W. (1999). Peroxisome proliferator-activated receptor alpha mediates the adaptive response to fasting. J. Clin. Invest. *103*, 1489–1498.

Kerver, E.D., Vogels, I.M., Bosch, K.S., Vreeling-Sindelárová, H., Van den Munckhof, R.J., and Frederiks, W.M. (1997). In situ detection of spontaneous superoxide anion and singlet oxygen production by mitochondria in rat liver and small intestine. Histochem. J. *29*, 229–237.

Koves, T.R., Ussher, J.R., Noland, R.C., Slentz, D., Mosedale, M., Ilkayeva, O., Bain, J., Stevens, R., Dyck, J.R., Newgard, C.B., et al. (2008). Mitochondrial overload and incomplete fatty acid oxidation contribute to skeletal muscle insulin resistance. Cell Metab. *7*, 45–56.

Lands, W.E. (1958). Metabolism of glycerolipides; a comparison of lecithin and triglyceride synthesis. J. Biol. Chem. *231*, 883–888.

Lauria, G., Lombardi, R., Borgna, M., Penza, P., Bianchi, R., Savino, C., Canta, A., Nicolini, G., Marmiroli, P., and Cavaletti, G. (2005). Intraepidermal nerve fiber density in rat foot pad: neuropathologic-neurophysiologic correlation. J. Peripher. Nerv. Syst. *10*, 202–208.

Liang, G., Yang, J., Horton, J.D., Hammer, R.E., Goldstein, J.L., and Brown, M.S. (2002). Diminished hepatic response to fasting/refeeding and liver X receptor agonists in mice with selective deficiency of sterol regulatory element-binding protein-1c. J. Biol. Chem. *277*, 9520–9528.

Liu, S., Brown, J.D., Stanya, K.J., Homan, E., Leidl, M., Inouye, K., Bhargava, P., Gangl, M.R., Dai, L., Hatano, B., et al. (2013). A diurnal serum lipid integrates hepatic lipogenesis and peripheral fatty acid use. Nature *502*, 550–554.

LoVerme, J., Russo, R., La Rana, G., Fu, J., Farthing, J., Mattace-Raso, G., Meli, R., Hohmann, A., Calignano, A., and Piomelli, D. (2006). Rapid broad-spectrum analgesia through activation of peroxisome proliferator-activated receptor-alpha. J. Pharmacol. Exp. Ther. *319*, 1051–1061.

Nave, K.A. (2010). Myelination and the trophic support of long axons. Nat. Rev. Neurosci. *11*, 275–283.

Nave, K.A., and Trapp, B.D. (2008). Axon-glial signaling and the glial support of axon function. Annu. Rev. Neurosci. *31*, 535–561.

Pollock, M., Nukada, H., Frith, R.W., Simcock, J.P., and Allpress, S. (1983). Peripheral neuropathy in Tangier disease. Brain *106*, 911–928.

Rogers, G.W., Brand, M.D., Petrosyan, S., Ashok, D., Elorza, A.A., Ferrick, D.A., and Murphy, A.N. (2011). High throughput microplate respiratory measurements using minimal quantities of isolated mitochondria. PLoS ONE *6*, e21746.

Roglio, I., Giatti, S., Pesaresi, M., Bianchi, R., Cavaletti, G., Lauria, G., Garcia-Segura, L.M., and Melcangi, R.C. (2008). Neuroactive steroids and peripheral neuropathy. Brain Res. Brain Res. Rev. *57*, 460–469.

Saher, G., Quintes, S., Möbius, W., Wehr, M.C., Krämer-Albers, E.M., Brügger, B., and Nave, K.A. (2009). Cholesterol regulates the endoplasmic reticulum exit of the major membrane protein P0 required for peripheral myelin compaction. J. Neurosci. *29*, 6094–6104.

Saher, G., Quintes, S., and Nave, K.A. (2011). Cholesterol: a novel regulatory role in myelin formation. Neuroscientist *17*, 79–93.

Stassart, R.M., Fledrich, R., Velanac, V., Brinkmann, B.G., Schwab, M.H., Meijer, D., Sereda, M.W., and Nave, K.A. (2013). A role for Schwann cell-derived neuregulin-1 in remyelination. Nat. Neurosci. *16*, 48–54.

Strable, M.S., and Ntambi, J.M. (2010). Genetic control of de novo lipogenesis: role in diet-induced obesity. Crit. Rev. Biochem. Mol. Biol. *45*, 199–214.

Taveggia, C., Zanazzi, G., Petrylak, A., Yano, H., Rosenbluth, J., Einheber, S., Xu, X., Esper, R.M., Loeb, J.A., Shrager, P., et al. (2005). Neuregulin-1 type III determines the ensheathment fate of axons. Neuron *47*, 681–694.

Van Veldhoven, P.P. (2010). Biochemistry and genetics of inherited disorders of peroxisomal fatty acid metabolism. J. Lipid Res. *51*, 2863–2895.

Verheijen, M.H., Chrast, R., Burrola, P., and Lemke, G. (2003). Local regulation of fat metabolism in peripheral nerves. Genes Dev. *17*, 2450–2464.

Verheijen, M.H., Camargo, N., Verdier, V., Nadra, K., de Preux Charles, A.S., Médard, J.J., Luoma, A., Crowther, M., Inouye, H., Shimano, H., et al. (2009). SCAP is required for timely and proper myelin membrane synthesis. Proc. Natl. Acad. Sci. USA *106*, 21383–21388.

Viader, A., Sasaki, Y., Kim, S., Strickland, A., Workman, C.S., Yang, K., Gross, R.W., and Milbrandt, J. (2013). Aberrant Schwann cell lipid metabolism linked to mitochondrial deficits leads to axon degeneration and neuropathy. Neuron *77*, 886–898.

Wassif, C.A., Zhu, P., Kratz, L., Krakowiak, P.A., Battaile, K.P., Weight, F.F., Grinberg, A., Steiner, R.D., Nwokoro, N.A., Kelley, R.I., et al. (2001). Biochemical, phenotypic and neurophysiological characterization of a genetic mouse model of RSH/Smith—Lemli—Opitz syndrome. Hum. Mol. Genet. *10*, 555–564.

Wierzbicki, A.S., Lloyd, M.D., Schofield, C.J., Feher, M.D., and Gibberd, F.B. (2002). Refsum's disease: a peroxisomal disorder affecting phytanic acid alpha-oxidation. J. Neurochem. *80*, 727–735.

Xu, H.E., Stanley, T.B., Montana, V.G., Lambert, M.H., Shearer, B.G., Cobb, J.E., McKee, D.D., Galardi, C.M., Plunket, K.D., Nolte, R.T., et al. (2002). Structural basis for antagonist-mediated recruitment of nuclear co-repressors by PPARalpha. Nature *415*, 813–817.

Yao, J.K., Holman, R.T., Lubozynski, M.F., and Dyck, P.J. (1980). Changes in fatty acid composition of peripheral nerve myelin in essential fatty acid deficiency. Arch. Biochem. Biophys. *204*, 175–180.